Reaction of the Anionic Acylmethylidyne Cluster $[Ru_3(CO)_9(\mu_3\text{-}CO)(\mu_3\text{-}CC(O)CH_3)]^-$ with CO and H_2: Reversible C–C and C–H Bond Forming Reactions

Michael J. Sailor, Michal Sabat, and Duward F. Shriver*

Department of Chemistry, Northwestern University, Evanston, Illinois 60208

Received August 20, 1987

The result of reaction of the acylmethylidyne cluster $[Ru_3(CO)_9(\mu_3\text{-}CO)(\mu_3\text{-}CC(O)CH_3)]^-$ (1) with either CO or H_2 is a cluster with an O→Ru bond between a metal vertex and the $C\text{-}C(O)CH_3$ moiety. In the reaction with CO a carbon–carbon bond is formed, producing the $\mu_2\text{-}\eta^2$-acyl cluster $[Ru_3(CO)_7(\mu\text{-}CO)_3(\mu_2\text{-}\eta^2\text{-}CH_3C(O)CCO)]^-$ (2). Similarly a carbon–hydrogen bond is formed on treatment of 1 with H_2, generating the $\mu_3\text{-}\eta^2$-acyl cluster $[HRu_3(CO)_9(\mu_3\text{-}\eta^2\text{-}CHC(O)CH_3)]^-$ (3). The reaction of 1 with CO is rapid and reversible, with an equilibrium constant at 20 °C of 2.1 (3) atm^{-1} (for 1 + CO ⇌ 2). The acylketenylidene cluster $[Ru_3(CO)_7(\mu\text{-}CO)_3(\mu_2\text{-}\eta^2\text{-}CH_3C(O)CCO)]^-$ (2) has been characterized in situ by variable-temperature and two-dimensional ^{13}C NMR spectroscopy. Isotopic tracer studies indicate the ketenyl CO of 2 originates from a cluster carbonyl on 1. Protonation of 3 occurs at ruthenium to generate $H_2Ru_3(CO)_9(\mu_3\text{-}\eta^2\text{-}CHC(O)CH_3)$ (4). The O→Ru interaction in compounds 2–4 can be readily disrupted. For example, the CO adduct $[Ru_3(CO)_7(\mu\text{-}CO)_3(\mu_2\text{-}\eta^2\text{-}CH_3C(O)CCO)]^-$ (2) reverts to $[Ru_3(CO)_9(\mu_3\text{-}CO)(\mu_3\text{-}CC(O)CH_3)]^-$ (1) on removal of CO, and the acetyl oxygen of $[HRu_3(CO)_9(\mu_3\text{-}\eta^2\text{-}CHC(O)CH_3)]^-$ (3) can be alkylated by $CH_3SO_3CF_3$ to give the previously characterized vinylidene cluster $H_2Ru_3(CO)_9(\mu_3\text{-}\eta^2\text{-}C{=}C(OCH_3)CH_3)$ (5). Treatment of 3 with DCl produces 4-d_1, which rapidly eliminates acetone-d_1. The benzyltrimethylammonium salt of 1 crystallizes in the orthorhombic space group $P2_12_12_1$ (No. 19) with a = 13.978 (5), b = 21.431 (7), and c = 9.224 (4) Å, V = 2763 (3) Å^3, and D(calcd) = 1.90 g cm^{-3} for mol wt 788.6 and Z = 4. Final discrepancy indices are R_F = 5.4% and R_{wF} = 7.4% for 1219 independent reflections with $I > 3\sigma(I)$.

Introduction

The tendency of an ensemble of metal atoms to stabilize a ligand through multicentered interactions is a distinguishing feature of metal cluster chemistry. For instance the symmetrically capping C–R group in alkylidyne clusters generally has a high degree of chemical stability.[1] In the present work, we investigate the reactivity of $[Ru_3(CO)_9(\mu_3\text{-}CO)(\mu_3\text{-}CC(O)CH_3)]^-$ (1), an acyl-substituted alkylidyne cluster that readily adds H_2 or CO to form C–H or C–C bonds with the apical carbon atom. In either case, the μ_3-bonding arrangement of the capping $C\text{-}C(O)CH_3$ group is replaced by one in which the oxygen atom of the acyl participates in bonding to the metal framework. Thus the ketonic group plays a role in determining the chemistry of this anionic alkylidyne cluster by providing an alternate bonding possibility.

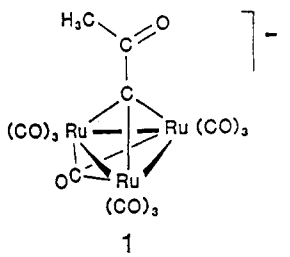

1

Experimental Section

General Information. All manipulations were carried out under vacuum or a dry dinitrogen atmosphere by using standard vacuum line, Schlenk, and syringe techniques or in a Vacuum Atmospheres drybox.[2] Solvents were distilled from the appropriate drying agents before use: CH_2Cl_2 and CD_2Cl_2 from P_2O_5 isopropyl ether and diethyl ether from sodium benzophenone ketyl. Carbon monoxide (Matheson, CP) and ^{13}CO (99%, Monsanto Research Co., Mound facility) were dried over activated silica gel before use. $CH_3SO_3CF_3$ (methyl trifluoromethanesulfonate, Aldrich) was distilled before use. Hydrogen (Matheson, UHP), $HBF_4{\cdot}Et_2O$ (Aldrich), D_2O (99.8%, Aldrich), and chromium(III) acetylacetonate (Aldrich) were used as received. Salts of $[Ru_3(CO)_9(\mu_3\text{-}CO)(\mu_3\text{-}CC(O)CH_3)]^-$ (1), $[Ru_3(*CO)_9(\mu_3\text{-}*CO)(\mu_3\text{-}*C*C(O)CH_3)]^-$, and $[Ru_3(CO)_9(\mu\text{-}CO)(\mu_3\text{-}*CC(O)CH_3)]^-$ were prepared as described previously (*C denotes ^{13}C enrichment of 20–60%).[3] The J_{CC} coupling constants reported in this work were obtained from the ^{13}C-enriched species in each case.

Infrared spectra were recorded on a Perkin-Elmer 283 grating infrared spectrophotometer or on a Nicolet 7199 fourier transform infrared spectrophotometer. A JEOL FX-270 or a Varian XL-400 spectrometer was used to record the ^1H and ^{13}C spectra. The ^1H and ^{13}C spectra were referenced to the residual solvent protons or carbon signal from the solvent, respectively, based on 0.0 ppm for $SiMe_4$. Mass spectra were obtained on a Hewlett-Packard 5985A operating in 70-eV electron-impact mode. The GC–MS spectra were obtained on the same instrument, using a 1.8 m × 2 mm stainless steel column packed with 10% Carbowax 400 on Chromosorb WHP (80–100 mesh, Alltech Assoc.). Preliminary GC traces were obtained with the same column on a Varian 3700 gas chromatograph under the following conditions: He flow rate, 20 cm^3/min; oven temperature, 40 °C; injector temperature, 220 °C; thermal conductivity detector, 200 °C. Elemental analyses were performed by Galbraith Laboratories.

Characterization of $[Ru_3(CO)_7(\mu\text{-}CO)_3(\mu_2\text{-}\eta^2\text{-}CH_3C(O)CCO)]^-$ (2). For the NMR experiments typically 50 mg of 1 was loaded into a 5-mm J. Young's, Inc., resealable NMR tube fitted with a concentric Teflon valve enabling it to be connected to a high vacuum line and ca. 0.5 mL of CD_2Cl_2 was vacuum transferred into the frozen solution. The desired amount of CO or ^{13}CO was introduced manometrically. The solutions were typically agitated for an hour to ensure complete equilibration. Following are the NMR signals for species 2; species 1 has been previously characterized:[3] ^1H NMR (CD_2Cl_2, 20 °C) 1.86 (s, CH_3) ppm; ^{13}C NMR (CD_2Cl_2, 20 °C) 227.7 (br, 7 CO's), 206.2 ($CH_3C(O)CCO$), 202.9 (br, CO), 200.9 (br, CO), 199.8 (CO), 166.0 ($CH_3C(O)CCO$), 30.7 ($CH_3C(O)CCO$), 30.3 ($CH_3C(O)CCO$) ppm; coupling constants (from ^{13}C enriched species—see text), 87 Hz ($^1J_{CC}$, $CH_3C(O)CCO$), 68 Hz ($^1J_{CC}$, $CH_3C(O)CCO$), 8 Hz ($^2J_{CC}$, $CH_3C(O)CCO$); ^{13}C NMR (CD_2Cl_2, −80 °C, carbonyls) 266.3, 266.2, 260.7, 202.1, 201.8, 200.1,

(1) Seyferth, D. *Adv. Organomet. Chem.* **1976**, *14*, 97.
(2) Shriver, D. F.; Drezdzon, M. A. *Manipulation of Air Sensitive Compounds*, 2nd ed.; Wiley: New York, 1986.
(3) Sailor, M. J.; Brock, C. P.; Shriver, D. F. *J. Am. Chem. Soc.* **1987**, *109*, 6015.

0276-7333/88/2307-0728$01.50/0 © 1988 American Chemical Society

199.8, 199.6, 199.2 (1:1:1:1:1:1:1:1:2) ppm. ^{13}C assignments were made by selective labeling experiments as described in the text.

For the ^{13}C COSY experiment, the sample preparation was the same as described above except that a 10-mm resealable NMR tube was used. The tube was charged with 130 mg (0.10 mmol) of 1-^{13}C (60% ^{13}C at $CC(O)CH_3$, ca. 20% at the carbonyls, and natural abundance at the CH_3), 50 mg of $Cr(Acac)_3$, 2 mL of CD_2Cl_2, and 0.3 mmol of 99% ^{13}CO. Spin–lattice relaxation times (T_1's) for the carbon resonances in the sample were determined,[4] the longest of which being 2.0 s for C(α) of **2**. The Varian instruments program COSY was used to acquire the spectrum.[5] Data acquisition required 7 h.

Equilibrium Constant for the Reaction 1 + CO ⇌ 2. K_{eq} was determined by NMR. In a typical experiment, a ca. 0.02 M solution of **1** was placed under CO in a 10-mm resealable NMR tube. The ratio [2]/[1] was measured as the ratio of the integrated methyl resonance of each species. The NMR tube was quickly frozen in liquid nitrogen and the amount of gas phase CO measured by Toeppler pump. The total free volume in the tube was determined separately, and so the pressure of CO in the tube, $P(CO)$, could be calculated. K_{eq} was calculated from eq 1.

$$K_{eq} = [2]/[1]P(CO) \quad (1)$$

Equilibration Rates of 1 + CO ⇌ 2 by Spin Saturation Transfer. The proton spin saturation transfer method of determining forward and reverse rate constants[6] was applied to the equilibrium mixture of **1** and **2** prepared in an NMR tube as described above. In a typical experiment, the $[Ru_3(CO)_9(\mu_3\text{-}CO)(\mu_3\text{-}CC(O)CH_3)]^-$ (**1**) methyl resonance was irradiated for $5T_1(\mathbf{2})$ and the integrated intensity of the methyl resonance of **2**, $M_\infty(\mathbf{2})$, was recorded. The integrated intensity of the CH_3 in **2** was then recorded after irradiation for $5T_1(\mathbf{2})$ at a position an equal frequency away from the methyl resonance of **2**, but on the side opposite the methyl resonance of **1**, providing $M_0(\mathbf{2})$. The value of k_1, the forward pseudo rate constant (uncorrected for [CO]), and of k_{-1} can be calculated from eq 2.[6]

$$k_1 = \frac{1}{T_1(\mathbf{2})}\left[\frac{M_0(\mathbf{2})}{M_\infty(\mathbf{2})} - 1\right] \quad (2)$$

Synthesis of $[HRu_3(CO)_9(\mu_3\text{-}\eta^2\text{-}CHC(O)CH_3)]^-$ (3). A flask containing a solution of 200 mg (0.16 mmol) of $[PPN][Ru_3(CO)_9(\mu_3\text{-}CO)(\mu_3\text{-}CC(O)CH_3)]^-$ (**1**) in 5 mL of CH_2Cl_2 was purged with H_2 several times, then charged to ca. 1 atm, and sealed off. The solution was stirred for 24 h with intermittent replacement of the atmosphere in the flask with fresh H_2. The solvent was removed and the yellow residue extracted into 2 mL of diethyl ether. Addition of 2 mL of isopropyl ether yielded yellow crystals of **3**, which were washed with small aliquots of isopropyl ether and dried in vacuo: yield 130 mg, 71%; IR (ν_{CO}, Et_2O) 2051 (w), 2027 (m), 2011 (s), 1992 (vs), 1960 (s), 1926 (w) cm^{-1}; ^1H NMR (CD_2Cl_2, 20 °C) 4.03 (s, 1 H, $CHC(O)CH_3$), 1.79 (s, 3 H, $CHC(O)CH_3$), −12.01 (s, 1 H, $Ru_2(\mu\text{-}H)$) ppm; ^{13}C NMR (CD_2Cl_2, −90 °C) 230.7 (1 C, $CHC(O)CH_3$), 206.2, 204.7 (br), 204.0, 200.3 (br), 191.7 (br) (1:2:2:2:2, terminal CO ligands), 77.5 (1 C, $CHC(O)CH_3$), 28.5 (1 C, $CHC(O)CH_3$) ppm; coupling constants, 46 Hz ($^1J_{CC}$, $CHC(O)CH_3$), 141 Hz ($^1J_{CH}$, $CHC(O)CH_3$). Anal. Calcd (Found) for $Ru_3C_{48}H_{35}O_{10}NP_2$: C, 50.09 (49.91); H, 3.06 (2.79); N, 1.22 (0.92); Ru, 26.35 (25.54).

Conversion of $[HRu_3(CO)_9(\mu_3\text{-}\eta^2\text{-}CHC(O)CH_3)]^-$ (3) to $H_2Ru_3(CO)_9(\mu_3\text{-}\eta^2\text{-}CHC(O)CH_3$ (4) and $H_2Ru_3(CO)_9(\mu_3\text{-}\eta^2\text{-}C{=}C(OCH_3)CH_3)$ (5). Both the protonation and the methylation of **3** were followed by ^1H NMR. In a typical experiment ca. 50 mg of $[HRu_3(CO)_9(\mu_3\text{-}\eta^2\text{-}CHC(O)CH_3)]^-$ (**3**) were loaded into a 5-mm NMR tube fitted with a rubber septum. After dissolution in ca. 0.5 mL of CD_2Cl_2, 1 equiv of either $HBF_4\cdot Et_2O$ or $CH_3SO_3CF_3$ was added by microliter syringe. The product of $HBF_4\cdot Et_2O$ addition (**4**) appeared immediately while that of $CH_3SO_3CF_3$ addition (**5**) grew in over several hours. No intermediates were detectable by ^1H NMR in either case. The ^1H NMR spectra of **4** and **5** matched those previously reported for these compounds.[3] In separate experiments the same reactions were carried out in CH_2Cl_2 solution in ordinary Schlenk ware and the infrared and mass spectra of the products agreed with the previously reported spectra in either case.[3] The presence of ca. 1 atm of CO over the solution had no detectable effect on the reaction of $CH_3SO_3CF_3$ with **3**.

Addition of DCl to $[HRu_3(CO)_9(\mu_3\text{-}\eta^2\text{-}CHC(O)CH_3)]^-$ (3) was done in a resealable 5-mm NMR tube and the appropriate amount of DCl added to the frozen CD_2Cl_2 solution of **3** from a calibrated gas bulb on a high vacuum line. The NMR spectrum recorded within 15 min of DCl addition showed primarily signals associated with $H_2Ru_3(CO)_9(\mu_3\text{-}\eta^2\text{-}CHC(O)CH_3)$, although the integrated ratio of the CH_3:CH:M–H:M–H protons was 3.00:0.68:0.78:0.78. After 45 min the signals for $H_2Ru_3(CO)_9(\mu_3\text{-}\eta^2\text{-}CHC(O)CH_3)$ had decreased significantly in intensity compared to the PPN counterion and residual solvent proton signals, and a resonance at 2.12 ppm had grown in. The presence of acetone-d_1 was confirmed by GC–MS of the reaction volatiles. Tabulation of the mass spectral data along with the predicted ion envelope patterns based on two statistical scrambling models for the D label are presented in the supplementary material.

Exposure of $[HRu_3(CO)_9(\mu_3\text{-}\eta^2\text{-}CHC(O)CH_3)]^-$ (3) to CO. One atmosphere of CO was introduced manometrically to a solution of 50 mg (0.04 mmol) of **3** in 0.5 mL of CD_2Cl_2 in a 5-mm resealable NMR tube. No change from the original ^1H NMR spectrum of **3** was observed after either 1 or 24 h of exposure of the solution of **3** to CO.

X-ray Data Collection and Structure Determination. Only small crystals of the benzyltrimethylammonium salt of $[Ru_3(CO)_9(\mu_3\text{-}CO)(\mu_3\text{-}CC(O)CH_3)]^-$ (**1**) could be obtained by slow diffusion of hexane into a diethyl ether solution. A crystal of dimensions 0.19 × 0.07 × 0.04 mm was mounted on a glass fiber and transferred to the cold stream (−120 °C) of an Enraf-Nonius CAD4 diffractometer. All measurements were performed by using Mo Kα radiation (λ = 0.71069 Å); lattice parameters were determined by the least-squares techniques applied to setting angles of 23 reflections. The systematic absences indicated uniquely the orthorhombic space group $P2_12_12_1$ (No. 19). The intensities of three standard reflections were measured every 3 h of X-ray exposure showing 9% decay. The data were corrected for Lorentz and polarization effects and the decay. The crystal diffracted rather weakly, and generally no significant intensities were observed during a scan of the range above 2θ = 45°.

All calculations were performed on a VAX 11/730 computer using the TEXSAN crystallographic program package.[7a] The structure was solved by direct methods (MITHRIL).[7b] Refinement was performed by full-matrix least-squares procedures with anisotropic thermal parameters for the Ru atoms. Most of the H atoms were located from difference Fourier maps. The position of the remaining H atoms were calculated by geometrical considerations assuming a C–H distance of 0.95 Å. The H atoms were included in the models as fixed contributors to the structure assuming isotropic thermal parameters of 1.2B(eqv) where B(eqv) are the temperature factors of the C atoms to which the H atoms were attached. The largest peak in the final difference electron density map (1.18 e/Å^3) was located near the Ru atoms. The goodness-of-fit was 1.09. Atomic scattering factors were those tabulated by Cromer and Waber[8a] with anomalous dispersion corrections taken from the literature.[8b] Refinement of the model with inverted coordinates led to the same values of the R factors and goodness-of-fit. Final positional parameters are presented in Table II.

Results

Spectroscopic Characterization of the Acyl-

(4) Sass, M.; Ziessow, D. *J. Magn. Reson.* **1977**, *25*, 263.
(5) Bax, A.; Freeman, R.; Morris, G. A. *J. Magn. Reson.* **1981**, *42*, 169.
(6) (a) Martin, M. L.; Martin, G. J.; Delpuech, J.-J. *Practical NMR Spectroscopy*; Heyden: London, 1980; Chapter 2. (b) Faller, J. W. In *Determination of Organic Structures by Physical Methods*; Nachod, F. C., Zuckerman, J. J., Ed.; Academic: New York, 1973; Vol. 5, Chapter 2.

(7) (a) Swepston, P. N. TEXSAN, Version 2.0, the TEXRAY Structure Analysis Program Package, Molecular Structure Corporation, College Station, TX, 1986. (b) Gilmore, G. N. MITHRIL, A computer program for the automatic solution of crystal structures from X-ray data; University of Glasgow: Glasgow, Scotland, 1983.
(8) (a) *International Tables for X-ray Crystallography*; Kynoch: Birmingham, England, 1974; Vol. 14, p 99. (b) *Ibid.*, p 149.

Table I. Summary of the Crystal Structure Data for $[Ru_3(CO)_9(\mu_3\text{-}CO)(\mu_3\text{-}CC(O)CH_3)]^-$ (1)

formula	$C_{23}H_{19}N_1O_{11}Ru_3$
fw	788.61
cryst system	orthorhombic
space group	$P2_12_12_1$ (No. 19)
a, Å	13.978 (5)
b, Å	21.431 (7)
c, Å	9.224 (4)
V, Å^3	2763 (3)
Z	4
d(calcd), g cm^{-3}	1.50
μ(Mo Kα), cm^{-1}	16.4
radiatn	graphite-monochromated Mo Kα (λ = 0.71069 Å)
scan type	$\theta/2\theta$
2θ range, deg	4–45
scan width, deg	0.7 + 0.35 tan θ
unique data	2078
unique data with $I > 3\sigma(I)$	1219
no. of parameters	169
$R(F)$	0.054
$R_w(F)$	0.074

Table II. Bond Distances and Angles for $[Ru_3(CO)_9(\mu_3\text{-}CO)(\mu_3\text{-}CC(O)CH_3)]^-$ (1)[a]

Intramolecular Distances Involving the Non-Hydrogen Atoms

atom	atom	dist	atom	atom	dist
Ru1	C11	1.86 (3)	Ru3	C2	2.05 (3)
Ru1	C13	1.90 (3)	Ru3	C1	2.15 (3)
Ru1	C12	1.94 (3)	O1	C1	1.29 (3)
Ru1	C1	2.05 (3)	O2	C3	1.24 (3)
Ru1	C2	2.08 (2)	O11	C11	1.19 (3)
Ru1	Ru3	2.777 (3)	O12	C12	1.12 (3)
Ru1	Ru2	2.786 (3)	O13	C13	1.18 (3)
Ru2	C23	1.87 (3)	O21	C21	1.15 (3)
Ru2	C21	1.91 (3)	O22	C22	1.11 (3)
Ru2	C22	1.99 (3)	O23	C23	1.19 (4)
Ru2	C2	2.14 (2)	O31	C31	1.16 (3)
Ru2	C1	2.21 (3)	O32	C32	1.16 (3)
Ru2	Ru3	2.755 (3)	O33	C33	1.15 (3)
Ru3	C31	1.85 (3)	C2	C3	1.43 (3)
Ru3	C33	1.90 (3)	C3	C4	1.52 (4)
Ru3	C32	1.92 (3)			

Intramolecular Bond Angles Involving the Non-Hydrogen Atoms

atom	atom	atom	angle	atom	atom	atom	angle
Ru3	Ru1	Ru2	59.37 (8)	O2	C3	C2	123 (2)
Ru3	Ru2	Ru1	60.15 (8)	O2	C3	C4	114 (3)
Ru2	Ru3	Ru1	60.48 (8)	C2	C3	C4	122 (2)
O1	C1	Ru1	135 (2)	O11	C11	Ru1	171 (3)
O1	C1	Ru3	132 (2)	O12	C12	Ru1	178 (3)
O1	C1	Ru2	127 (2)	O13	C13	Ru1	178 (3)
C3	C2	Ru3	134 (2)	O21	C21	Ru2	177 (3)
C3	C2	Ru1	129 (2)	O22	C22	Ru2	174 (3)
C3	C2	Ru2	127 (2)	O23	C23	Ru2	175 (3)
Ru3	C2	Ru1	85 (1)	O31	C31	Ru3	171 (3)
Ru3	C2	Ru2	82.2 (9)	O32	C32	Ru3	174 (2)
				O33	C33	Ru3	177 (2)

[a] Distances are in angstroms and angles in degrees. Estimated standard deviations in the least significant Figure are given in parentheses.

ketenylidene $[Ru_3(CO)_7(\mu\text{-}CO)_3(\mu_2\text{-}\eta^2\text{-}CH_3C(O)CCO)]^-$ (2). An equilibrium is established between 1 and 2 in methylene chloride solution according to eq 3. The

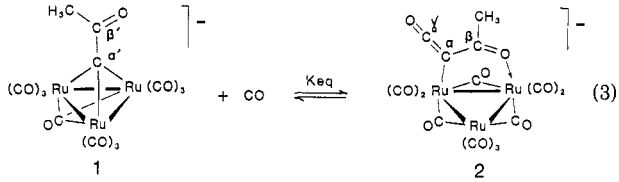

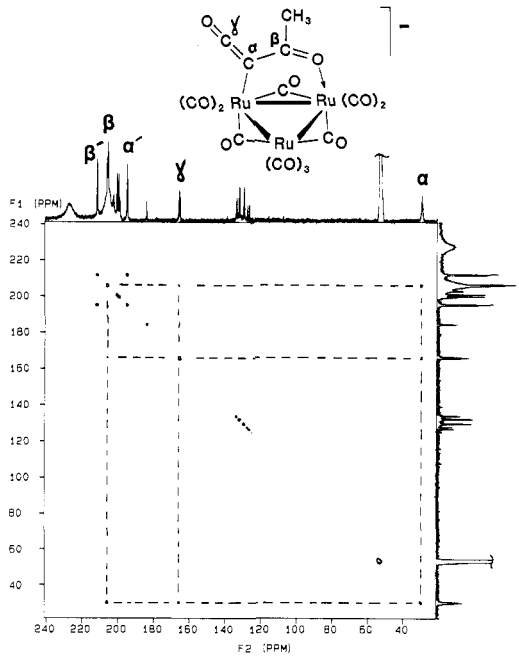

Figure 1. Homonuclear ^{13}C (100.57-MHz) 2D-COSY spectrum of the equilibrium mixture of $[Ru_3(CO)_9(\mu_3\text{-}CO)(\mu_3\text{-}CC(O)CH_3)]^-$ (1) and $[Ru_3(CO)_7(\mu\text{-}CO)_3(\mu_2\text{-}\eta^2\text{-}CH_3C(O)CCO)]^-$ (2) establishing the connectivity of the acylketene ligand of 2. Every cluster carbon atom is ^{13}C enriched by at least 60% except for the CH_3 carbons, which are a natural abundance. Scalar one- and two-bond couplings give rise to the off-diagonal peaks. The resonances marked α^1 and β^1 are from species 1; α, β, and γ are from species 2. The peak at ca. 184 ppm is dissolved CO, those between 120 and 140 ppm are from the PPN^+ counterion, and the resonance at ca. 54 ppm is from the solvent.

equilibrium constant for the reaction at 20 °C was measured by ^1H NMR integration and manometric measurement of CO pressure, and a value of 2.1 (3) atm^{-1} was obtained as the average of six separate runs. The product of CO addition to 1, formulated as the acylketenylidene 2, readily reverts to 1 on removal of CO and could not be isolated in crystalline form. Thus, the CO adduct 2 was characterized by a series of NMR experiments. To establish the connectivity of the capping acylketene ligand, a ^{13}C–^{13}C COSY spectrum was obtained. In this experiment, the NMR spectrum of highly ^{13}C-enriched $[Ru_3(*CO)_9(\mu_3\text{-}*CO)(\mu_3\text{-}*C*C(O)CH_3)]^-$ under an atmosphere of ^{13}CO contained resonances of 1 and 2, as shown in Figure 1. In this experiment the methyl carbon was unenriched. Cross peaks arising from J_{CC} coupling between the highly ^{13}C-enriched carbon atoms are readily discerned for both species 1 and 2. The resonances for the precursor complex 1, labeled α' and β' in Figure 1, are known from previous work.[3] The resonances for the acylketenylidene ligand of 2 are labeled α, β, and γ, corresponding to the structure shown in Figure 1.

In a separate NMR experiment the individual CC coupling constants were measured: $^1J(\alpha'\beta') = 44$ Hz, $^1J(\alpha\beta) = 67$ Hz, $^1J(\alpha\gamma) = 87$ Hz, $^2J(\beta\gamma) = 8$ Hz. The assignments were made from NMR spectra on selectively ^{13}C-labeled molecules. Thus the equilibrium mixture of 1 and 2 under ^{13}CO contains the γ resonance at 166.0 ppm and the metal carbonyl resonances but not the α', β', α, or β resonances when normal isotopic 1 is used as the starting material. Similarly when 1 had been selectively enriched at α' and then equilibrated with ^{12}CO gas, the spectrum contained only resonances associated with α' and α. Finally, 1 enriched at both the α' and β' sites showed only the resonances α', β', α, and β under ^{12}CO. The positions of resonances α and γ in the ^{13}C NMR spectrum, assigned to

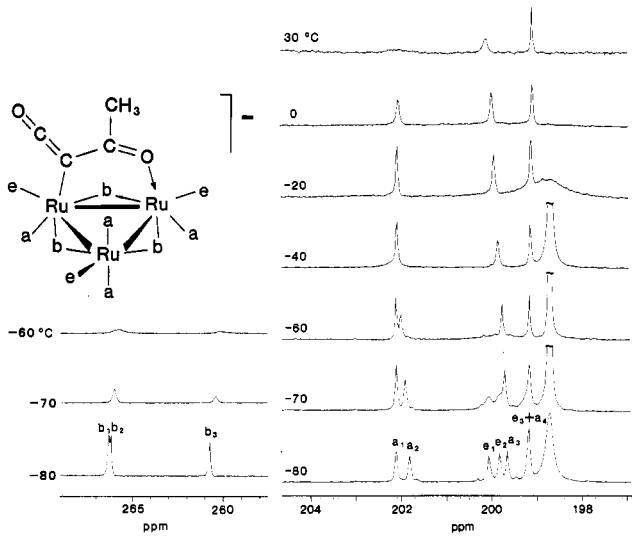

Figure 2. Variable-temperature ^{13}C (100.57-MHz) spectrum showing the carbonyl ligand fluxionality of $[Ru_3(CO)_7(\mu\text{-}CO)_3(\mu_2\text{-}\eta^2\text{-}CH_3C(O)CCO)]^-$ (**2**). The large peak on the far right of the −80 °C spectrum (not marked) is from the terminal carbonyl ligands of $[Ru_3(CO)_9(\mu_3\text{-}CO)(\mu_3\text{-}CC(O)CH_3)]^-$ (**1**). Only the CO ligands were ^{13}C enriched in these spectra.

the ketene moiety of **2**, are very similar to those observed for CCO ligands in other clusters. For example, the two ^{13}C signals for CCO in $[HRu_3(CO)_9(\mu_3\text{-}CCO)]^-$ are at 50.1 and 165.1 ppm, and in $H_2Ru_3(CO)_9(\mu_3\text{-}CCO)$ they are at 38.7 and 158.8 ppm.[3] In **2** the corresponding resonances for carbons α and γ are at 30.3 and 166.0 ppm, respectively. Additionally the carbon–carbon coupling constant for the CCO in **2** is comparable to that found in the previous two examples; for **2** $^1J_{\alpha\gamma}$ is 87 Hz and for either $[HRu_3(CO)_9(\mu_3\text{-}CCO)]^-$ or $H_2Ru_3(CO)_9(\mu_3\text{-}CCO)$ $^1J_{CC}$ for the $^{13}C^{13}CO$ ligand is 78 Hz.[3] The proton NMR spectrum of the equilibrium mixture of **1** and **2** contains a signal at 2.36 ppm for the methyl group of **1** and one at 1.87 ppm for the methyl group of **2**. The 1.87 ppm resonance is in a similar position to that of the $\mu_3\text{-}\eta^2$ ligand $CHC(O)CH_3$ in the clusters $[HRu_3(CO)_9(\mu_3\text{-}\eta^2\text{-}CHC(O)CH_3)]^-$ and $H_2Ru_3(CO)_9(\mu_3\text{-}\eta^2\text{-}CHC(O)CH_3)$.[3]

The carbonyl ligand fluxionality of **1** and **2** was investigated by variable-temperature NMR on samples enriched only at the carbonyl carbons (Figure 2). The interpretation of these spectra is simplified by spin saturation transfer experiments, discussed later, which indicate that the rates of interconversion of **1** ⇌ **2** are sufficiently slow with respect to the NMR time scale that **1** and **2** can be treated as independent species. The variable-temperature behavior of the NMR spectrum of **1** is simple and is therefore readily separated from the more complex CO fluxional pattern of **2**. At low temperature two CO resonances are observed for the one bridging (273.3 ppm) and nine terminal (198.7 ppm) CO ligands of $[Ru_3(CO)_9(\mu_3\text{-}CO)(\mu_3\text{-}CC(O)CH_3)]^-$ (**1**). When the temperature is raised to 20 °C, bridge–terminal exchange becomes fast on the NMR time scale, resulting in a single broad resonance at 206.2 ppm.

The exchange-frozen spectrum of $[Ru_3(CO)_7(\mu\text{-}CO)_3(\mu_2\text{-}\eta^2\text{-}CH_3C(O)CCO)]^-$ (**2**) is obtained at −80 °C. At this temperature, three bridging and six terminal CO resonances are observed, in a 1:1:1:1:1:1:1:1:2 pattern, indicating that the molecule has C_1 symmetry with two of the resonances (e_3 + a_4 in Figure 2) accidentally coincident. A structure consistent with the NMR results is shown in Figure 2. The peaks b_1, b_2, b_3, e_1, e_2, and e_3 simultaneously collapse on raising the temperature from −80 °C. By 0 °C a very broad resonance centered at 231 ppm is evident (not shown in Figure 2), corresponding closely to the average of the six resonances which have collapsed (232.1 ppm). We interpret this to be a "merry-go-round" exchange occurring between the three bridging carbonyls (b) and the three equatorial CO ligands (e) of the proposed structure. The four remaining CO ligands are disposed in axial positions on the cluster, and each has a different activation barrier for entering into the CO exchange process. Thus resonances a_1, a_2, a_3, and a_4 broaden more slowly on raising the temperature. Although a slight temperature dependence of the chemical shift causes resonance a_2 to be obscured by resonance a_1, by 0 °C integrations of the peaks indicate that a_2 has broadened into the base line. By +30 °C a broad peak for the average of resonances b_1, b_2, b_3, e_1, e_2, e_3, and a_2 is observed at 228 ppm (average of b_1, b_2, b_3, e_1, e_2, e_3, and a_2 in the −80 °C spectrum is 227.7 ppm). At +30 °C, the highest temperature studied, resonance a_1 has almost completely broadened into the base line, resonance a_3 has started to broaden, and resonance a_4 is still sharp. Thus at low temperature the static CO ligand geometry of **2** is observed, and as the temperature is increased, the bridging to equatorial carbonyl ligand exchange is seen, as well as the entrance of one of the axial CO ligands into metal-site exchange within the cluster. The NMR results are fully consistent with the proposed structure.

Low-Temperature Addition of ^{13}CO to $[Ru_3(CO)_9(\mu_3\text{-}CO)(\mu_3\text{-}CC(O)CH_3)]^-$ (1). In order to determine the origin of the CCO group on the acylketene ligand of **2**, the addition of ^{13}CO to **1** was monitored by ^{13}C NMR at low temperature. In this experiment ^{13}CO (99% isotopic purity) was introduced over a frozen solution of unenriched **1** in an NMR tube. The tube was thawed, shaken to dissolve the ^{13}CO, and quickly inserted into the NMR probe, which had been precooled to −70 °C. A spectrum was acquired within 30 min, although spectra taken 1 and 2 h later were only slightly different. Under these conditions signals for the metal-bound CO ligands of **2** were observed but the signal for the ketene CO of the $\mu_2\text{-}\eta^2\text{-}CH_3C(O)CCO$ ligand at 166.0 ppm was not. When the sample was allowed to sit at room temperature for 10 min before insertion into the probe cooled to −70 °C, the 166.0 ppm signal for the CCO moiety of **2** was evident in the ^{13}C NMR spectrum, and after the sample was allowed to sit at room temperature for 1 h, the integrated intensity of the acylketene CO signal indicated that full equilibration with the metal-bound CO's of **2** had occurred. The data indicate that the labeled CO is incorporated into the pool of metal-bound carbonyls but that the acylketene ligand is formed by coupling of the $\mu_3\text{-}CC(O)CH_3$ moiety with an original unlabeled cluster CO. Thus the kinetic product of ^{13}CO addition to **1** is **2** with no ^{13}C in the $\mu_2\text{-}\eta^2\text{-}CH_3C(O)CCO$ ligand. As the equilibrium of eq 3 is established, ^{13}CO is scrambled throughout the metal-bound CO ligands of **1** and **2** *and* the ketene CO of $CH_3C(O)CCO$.

Rates of Interconversion of 1 and 2. Spin saturation transfer experiments were performed in an attempt to measure the rates of the forward and reverse reaction represented by eq 3. At room temperature no magnetization transfer was observed between the methyl group of **1** and that of **2**. A similar experiment run at 40 °C also resulted in no measurable magnetization transfer in either direction. From the T_1 values and an estimate of the accuracy of our ability to measure the peak integrals, upper limits for both k_1 and k_{-1} are estimated to be $k_1[CO] < 3 \times 10^{-2}$ s^{-1} and $k_{-1} < 2 \times 10^{-1}$. Thus the half-life for decarbonylation of **2** is greater than 35 s. In separate ex-

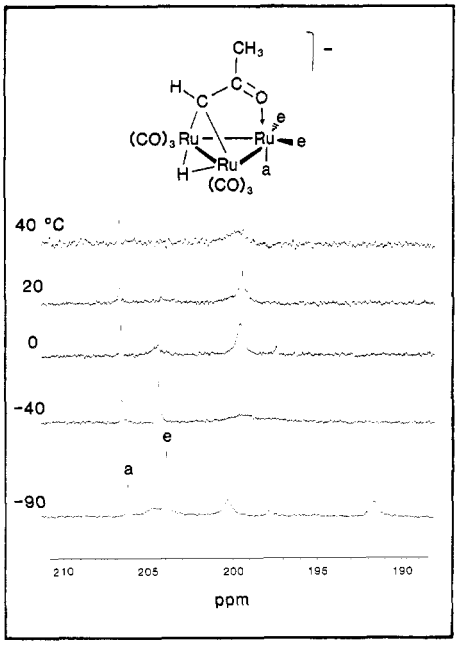

Figure 3. Variable-temperature ^{13}C (100.57 MHz) spectrum showing the carbonyl ligand fluxionality of $[HRu_3(CO)_9(\mu_3\text{-}\eta^2\text{-}CHC(O)CH_3)]^-$ (**3**). Acetonitrile was the solvent for data collected at +20 and +40 °C; in all other cases CD_2Cl_2 was used. Sample decomposition occurred above 50 °C.

periments the spin transfer method was applied to the equilibrium mixture of **1** and **2** in a saturated CD_2Cl_2 solution of lithium triflate. No magnetization transfer was observed at either room temperature or 40 °C.

Decomposition of $[Ru_3(CO)_7(\mu\text{-}CO)_3(\mu_2\text{-}\eta^2\text{-}CH_3C(O)CCO)]^-$ (2): Reaction with H_2O. The equilibrium solution of **1** and **2** under CO is stable for weeks. However, when traces of water are present, a slow reaction occurs over several days to form ultimately $Ru_3(CO)_{12}$ and $(CH_3)_2CO$ as well as a small amount of cluster anion, presumably $[HRu_3(CO)_{11}]^-$. The $Ru_3(CO)_{12}$ that crystallized from the solution was identified by IR and ^{13}C NMR spectroscopy as well as by an inadvertent X-ray crystal structure determination. The acetone produced was observed in situ by ^1H and ^{13}C NMR and also by GC–MS of the volatiles. When D_2O was added to a CH_2Cl_2 solution of **1** over CO and stirred for several days, the mass spectrum contained the parent ion for acetone-d_3 at 61 amu. Principle fragmentation peaks at 46 and 43 amu, corresponding to the fragments $CD_3C(O)$ and $CH_3C(O)$, respectively, along with smaller peaks at 58, 59, 60 and 62 amu for the d_0, d_1, d_2, and d_4 isotopomers were apparent in the mass spectrum.

Reaction of $[Ru_3(CO)_9(\mu_3\text{-}CO)(\mu_3\text{-}CC(O)CH_3)]^-$ (1) with Dihydrogen: Characterization of $[HRu_3(CO)_9(\mu_3\text{-}\eta^2\text{-}CHC(O)CH_3)]^-$ (3). When a methylene chloride solution of **1** is stirred under an atmosphere of H_2 for 24 h, the μ_3-η^2-acetyl cluster $[HRu_3(CO)_9(\mu_3\text{-}\eta^2\text{-}CHC(O)CH_3)]^-$ (**3**) formed, which was characterized spectroscopically and by elemental analysis. The ^1H NMR spectrum contains three resonances in a 1:3:1 integrated ratio corresponding to the C–H (4.03 ppm), CH_3 (1.79 ppm), and bridging hydride (−12.01 ppm) protons. The formation of a C–H bond in the reaction is confirmed by the ^{13}C resonance at 77.5 ppm, which is a doublet in the proton-coupled ^{13}C NMR spectrum ($^1J_{CH}$ = 141 Hz). Additionally, the 141 Hz $^1J_{CH}$ satellites are apparent on the 4.03 ppm ^1H NMR resonance in a sample of ^{13}C-enriched **3**.

The variable-temperature ^{13}C NMR spectra of **3** in the metal carbonyl region are presented in Figure 3. The spectra are interpreted in terms of two separate carbonyl exchange processes occurring with different activation energies. At low temperature two sharp resonances in a 1:2 intensity ratio as well as three broad resonances of roughly equal area are observed. The low-temperature spectrum is indicative of C_s symmetry, with the two sharp resonances a and e assigned to the one axial and two equatorial CO ligands on the unique ruthenium atom and the three broad resonances assigned to the three sets of symmetry related pairs of CO molecules on the other two Ru centers (see Figure 3). The lowest energy CO exchange process observed is the intramolecular turnstile interchange of the carbonyls attached to the symmetry-related pair of ruthenium atoms. Thus the three broad resonances present in the spectrum at −90 °C coalesce by −40 °C into a single resonance, representing all six of the carbonyl ligands not attached to the unique ruthenium. When the temperature is raised to 20 °C, the second CO exchange process is observed, namely, the broadening of resonance e corresponding to the two equatorial carbonyls on the unique ruthenium of **3**. Presumably these CO ligands are undergoing inter-metal exchange with the six carbonyls on the other Ru centers because the signal for the six CO's also broadens when the temperature is raised past 20 °C. The resonance a, assigned to the unique CO trans to the acetyl O→Ru interaction, is slightly broadened at +60 °C. Full coalescence of the ^{13}C NMR CO signals could not be observed, however, as appreciable decomposition of the sample occurred in CD_3CN above 50 °C. The ^1H NMR of **3** contains a single hydride resonance that remains sharp over the temperature range −90 to +20 °C.

Protonation of $[HRu_3(CO)_9(\mu_3\text{-}\eta^2\text{-}CHC(O)CH_3)]^-$ (3) To Generate $H_2Ru_3(CO)_9(\mu_3\text{-}\eta^2\text{-}CHC(O)CH_3)$ (4). Acidification of a methylene chloride solution of the monoanion **3** produces the previously characterized neutral cluster **4**, the result of simple protonation of $[HRu_3(CO)_9(\mu_3\text{-}\eta^2\text{-}CHC(O)CH_3)]^-$ on the metal framework.[3] No intermediates or side products could be detected on reaction of **3** with $HBF_4{\cdot}Et_2O$ at −40 °C by ^1H NMR. Protonation causes very little perturbation of the ^1H and ^{13}C NMR signals associated with the μ_3-η^2-$CHC(O)CH_3$ ligand, although the low-temperature ^{13}C NMR spectrum in the carbonyl region reflects the lower symmetry of **4** relative to **3**. Thus at low-temperature nine CO resonances are observed for $H_2Ru_3(CO)_9(\mu_3\text{-}\eta^2\text{-}CHC(O)CH_3)$ (**4**), consistent with a molecular symmetry of C_1 (Figure 4). When the temperature is raised, eight of the nine resonances collapse and eventually coalesce to four new resonances, indicating that at high temperature the molecule possesses a dynamic mirror plane on the NMR time scale. The variable-temperature ^{13}C NMR results shown in Figure 4 can be described by a single activation barrier ($\Delta G^{\ddagger}$) of 11.8 ± 0.7 kcal mol^{-1}, based on a simple line-shape analysis.[9] The apparent CO fluxionality might be explained by invoking hydride mobility on a static metal carbonyl cluster framework. However, the activation barrier for equilibration of the two hydride ligands calculated from the variable-temperature ^1H NMR spectrum of $H_2Ru_3(CO)_9(\mu_3\text{-}\eta^2\text{-}CHC(O)CH_3)$ is higher, 14.6 ± 0.7 kcal mol^{-1} (the errors quoted are at the 99% confidence level). Therefore, the fluxionality observed in the ^{13}C NMR arises from a process lower in energy than complete hydride exchange and is interpreted as the hopping of only one of the hydrides between the two metal–metal bonds related by the mirror plane. Keister et al. studied the dynamic NMR

(9) Sandström, J. *Dynamic NMR Spectroscopy*; Academic: London, 1982; Chapter 7.

spectra of a compound closely related to **4**, $H_2Ru_3(CO)_9(\mu_3\text{-}\eta^2\text{-}CHC(O)OCH_3)$,[10] and presented the interpretation described above.

Although **3** cleanly protonates to **4**, the latter is sensitive to the counterion of the acid. Complex **4** is stable in methylene chloride solutions containing BF_4^-, but apparently Cl^- promotes elimination of acetone from the cluster. Thus treatment of **3** with 1 equiv of DCl produces **4** initially, but within several minutes a peak at 2.12 ppm in the ^1H NMR begins to grow in at the expense of the signals for **4**. GC–MS analysis of the reaction volatiles confirms the presence of acetone-d_1. The mass spectra indicate that some intramolecular scrambling of the D atom has occurred.

Discussion

Reversible Reaction of $[Ru_3(CO)_9(\mu_3\text{-}CO)(\mu_3\text{-}CC(O)CH_3)]^-$ with CO: Formation of the Acylketene Cluster $[Ru_3(CO)_7(\mu\text{-}CO)_3(\mu_2\text{-}\eta^2\text{-}CH_3C(O)CCO)]^-$. The synthesis of $[Ru_3(CO)_9(\mu_3\text{-}CO)(\mu_3\text{-}CC(O)CH_3)]^-$ (**1**) from the ketenylidene cluster $[Ru_3(CO)_6(\mu\text{-}CO)_3(\mu_3\text{-}CCO)]^{2-}$ and methyl iodide is most efficiently carried out under an atmosphere of CO. Details of the probable mechanism of this reaction have been discussed by us previously.[3] It was during these studies that we noticed that the solution infrared spectrum of **1** was different if the solution was saturated with CO. Further investigation revealed that **1** establishes an equilibrium at room temperature which can readily be reversed by removal of the CO. The product of addition of CO to **1** was extensively characterized by NMR spectroscopy and is formulated as the acylketenylidene **2** (eq 4). An interesting feature of the reaction is that the addition of CO to cluster **1** triggers a CC bond forming reaction between the alkylidyne ligand and another carbonyl. Kinetically controlled carbon-13 labeling establishes that the ketenyl CO of **2** is not derived directly from the added CO, although eventually it does exchange with exogenous CO.

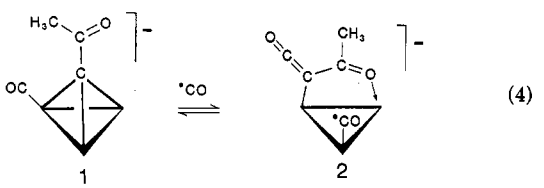

1 2 (4)

At room temperature the equilibrium is established within minutes, although in the range of concentrations and CO pressures studied, the forward and reverse rates were not fast enough to be studied by spin saturation transfer in the NMR. Such readily reversible CO addition to an alkylidyne cluster is rare, but there is a large number of examples of irreversible CO addition reactions on clusters and a few which can be driven in one direction or another under forcing conditions.[13,14] A situation closely related to the present one has been observed recently in the μ-methylene clusters $[Os_3(CO)_{10}(\mu\text{-}CH_2)(\mu\text{-}X)]^-$ (X = Cl, Br, I, NCO).[15] These clusters reversibly add CO under mild conditions to form the μ-ketene clusters $[Os_3(CO)_{10}(\mu\text{-}CH_2CO)(\mu\text{-}X)]^-$. Labeling studies indicate that one of the original cluster CO ligands undergoes insertion to form the μ-CH_2CO group. Thus the reaction is similar to the CO insertion presented in this work in that CO addition and CO insertion are occurring as separate events. Although the tracer experiments prove that the CO that inserts to form a carbon–carbon bond is not the same CO that adds to the cluster, it is unclear which process occurs first. The fact that the external CO is not immediately incorporated into the CCO indicates that C–C coupling may occur before CO addition, but we cannot rule out CO addition to the cluster followed by C–C coupling before the added CO has time to scramble throughout the molecule. In addition to these analogies in cluster chemistry cited above, there are examples of CO addition to carbon centers in mononuclear complexes containing carbene, carbyne, and acetylidene ligands.[14g-j]

Scheme I

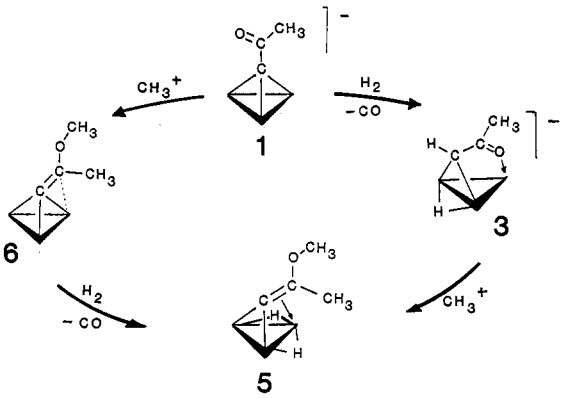

Reaction of $[Ru_3(CO)_9(\mu_3\text{-}CO)(\mu_3\text{-}CC(O)CH_3)]^-$ (1) with H_2. The O→Ru Interaction. The acetyl group of $[Ru_3(CO)_9(\mu_3\text{-}CO)(\mu_3\text{-}CC(O)CH_3)]^-$ (**1**) participates in the CO insertion process of eq 4 by entering into a bonding interaction with a ruthenium center. The ambident nature that the acetyl oxygen imparts to the capping group apparently distinguishes **1** from normal alkylidyne clusters, which do not display a large tendency to insert CO.[16] The oxygen atom of the acetyl group plays a similar role in the hydrogenation of **1**. Under mild conditions $[Ru_3(CO)_9(\mu_3\text{-}CO)(\mu_3\text{-}CC(O)CH_3)]^-$ reacts with H_2 to produce $[HRu_3(CO)_9(\mu_3\text{-}\eta^2\text{-}CHC(O)CH_3)]^-$ (eq 5). In the process of adding one H atom to the metals and one to the alkylidyne apical carbon, a bond forms between the acyl oxygen atom and a metal center. It is noteworthy that in this reaction CO is given off, and even under ca. 1 atm of CO the Ru–O bond appears to be left intact. Thus the acyl

(10) Churchill, M. R.; Janik, T. S.; Duggan, T. P.; Keister, J. B. *Organometallics* **1987**, *6*, 799.

(11) *Tables of Interatomic Distances and Configuration in Molecules and Ions, Supplement*; Sutton, L. E., Ed.; The Chemical Society: London, 1965.

(12) Churchill, M. R.; Hollander, F. J.; Hutchinson, J. P. *Inorg. Chem.* **1977**, *16*, 2655.

(13) Sappa, E.; Tiripicchio, A.; Braunstein, P. *Chem. Rev.* **1983**, *83*, 203.

(14) (a) Nuel, D.; Dahan, F.; Mathieu, R. *Organometallics* **1985**, *4*, 1436. (b) Horvath, I. T.; Zsolnai, L.; Huttner, G. *Organometallics* **1986**, *5*, 180. (c) Field, J. S.; Haines, R. J.; Smit, D. N.; Natarajan, K.; Scheidsteger, O.; Huttner, G. *J. Organomet. Chem.* **1982**, *240*, C23. (d) Jeffery, J. C.; Lawrence-Smith, J. G. *J. Chem. Soc., Chem. Commun.* **1986**, 17. (e) Morrison, E. D.; Steinmetz, G. R.; Geoffroy, G. L.; Fultz, W. C.; Rheingold, A. R. *J. Am. Chem. Soc.* **1984**, *106*, 4783. (f) Bavaro, L. M.; Montangero, P.; Keister, J. B. *J. Am. Chem. Soc.* **1983**, *105*, 4977. (g) Bodnar, T. W.; Cutler, A. R. *J. Am. Chem. Soc.* **1983**, *105*, 5926. (h) Herrmann, W. A.; Plank, J. *Angew. Chem., Int. Ed. Engl.* **1978**, *17*, 525. (i) Kreissl, F. R.; Friedrich, P.; Huttner, G. *Angew Chem., Int. Ed. Engl.* **1977**, *16*, 102. (j) Jeffrey, J. C.; Laurie, J. C. V.; Moore, I.; Stone, F. G. A. *J. Organomet. Chem.* **1983**, *258*, C37.

(15) Morrison, E. D.; Geoffroy, G. L. *J. Am. Chem. Soc.* **1985**, *107*, 3541.

(16) Duggan, T. P.; Barnett, D. J.; Muscatella, M. J.; Keister, J. B. *J. Am. Chem. Soc.* **1986**, *108*, 6076.

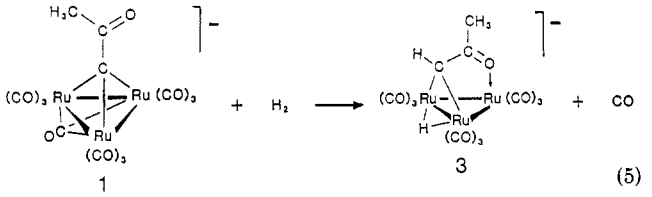

(5)

O→Ru interaction is favored over a Ru–CO bond. In an attempt to probe the tenacity of the Ru–O linkage, we reacted the anion **3** with methyl triflate. Alkylation at the oxygen occurs within hours to produce the previously characterized[3] vinylidene dihydride cluster $H_2Ru_3(CO)_9(\mu_3\text{-}CC(OCH_3)CH_3)$ (**5**). Thus although not readily dis-

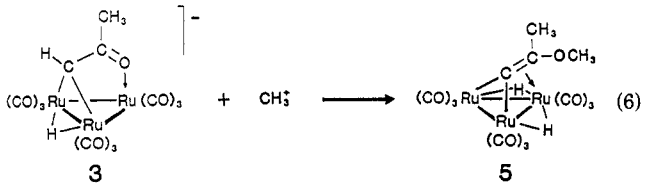

(6)

placed by CO, the acetyl O–metal interaction can be disrupted by a strong alkylating agent. The surprising feature of this transformation is that it proceeds with concomitant migration of the C-bonded proton to the metal framework. The C–H bond cleavage is facilitated by the formation of the $\mu_3\text{-}\eta^2$ vinylidene, apparently a highly stable moiety in trinuclear metal clusters.[13] Scheme I summarizes the role the acetyl group plays in this system. When the O atom of the acetyl is bonded to a metal center, C–H bond formation is preferred. If the ketonic oxygen of the acetyl ligand has been alkylated, the proton is more stable in $\mu\text{-}HRu_2$ positions.

Although oxophilic behavior is generally associated with the early transition metals, there are many examples from the iron triad of O-bonded acyls.[17] A pertinent example is found in the chemistry of $H_3Ru_3(CO)_9(\mu_3\text{-}CC(O)OCH_3)$, which rearranges upon pyrolysis to form $HRu_3(CO)_9(\mu_3\text{-}\eta^2\text{-}CHC(O)OCH_3)$ (eq 7).[10] The product of the reaction

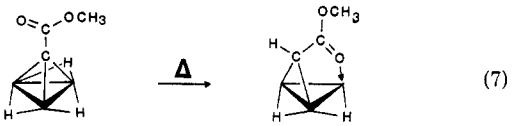

(7)

is a close relative of the clusters **3** and **4** reported in this work. It is intriguing that in the room-temperature conversion of $[Ru_3(CO)_9(\mu_3\text{-}CO)(\mu_3\text{-}CC(O)CH_3)]^-$ (**1**) to $[HRu_3(CO)_9(\mu_3\text{-}\eta^2\text{-}CHC(O)CH_3)]^-$ (**3**) (eq 5) we do not isolate a dihydride such as $[H_2Ru_3(CO)_9(\mu_3\text{-}CC(O)Me)]^-$, even though $H_3Ru_3(CO)_9(\mu_3\text{-}CC(O)OMe)$ requires heating for 24 h at 70 °C to effect the conversion to $H_2Ru_3(CO)_9(\mu_3\text{-}\eta^2\text{-}CHC(O)OMe)$ (eq 7).[10] It is evident that the activation barrier for C–H bond formation in eq 5 is lower than that in eq 7, although the factors controlling this difference have not yet been determined.

Protonation of $[HRu_3(CO)_9(\mu_3\text{-}\eta^2\text{-}CHC(O)CH_3)]^-$ (3). The acetyl clusters having O interactions with the metal

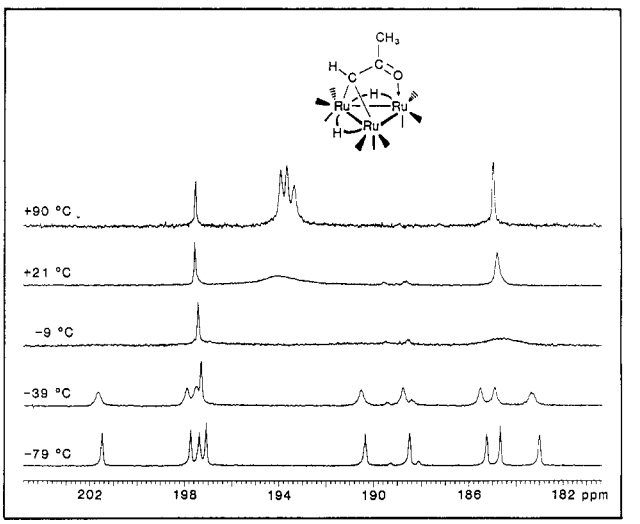

Figure 4. Variable-temperature ^{13}C (100.57 MHz) spectrum showing the carbonyl ligand fluxionality of $H_2Ru_3(CO)_9(\mu_3\text{-}\eta^2\text{-}CHC(O)CH_3)$ (**4**). Toluene-d_8 was the solvent for data collected at +90 °C; in all other cases CD_2Cl_2 was the solvent. Unlike the fluxional behavior of **3**, which is interpreted in terms of intra- and intermetal intramolecular CO exchange, the fluxionality of **4** is interpreted as arising from mobility of one of the hydride ligands on the metal framework (see text).

centers such as **2** and **3** suggest a pathway for metal-mediated C–O bond cleavage via O-bonded acetyls. Indeed, ketones O-bonded to zinc have been proposed as intermediates in the Clemensen reduction, a heterogeneous reaction which converts ketones to alkanes in the presence of amalgamated zinc and HCl.[18] In addition, reduction of the ketone functionality in the cobalt acetyl clusters $Co_3(CO)_9(\mu_3\text{-}CC(O)R)$ results in the formal abstraction of O to produce the alkylidyne clusters $Co_3(CO)_9(\mu_3\text{-}CCH_2R)$.[19] However, we have not observed C–O cleavage in the reactions of $H_2Ru_3(CO)_9(\mu_3\text{-}\eta^2\text{-}CHC(O)CH_3)$. Protonation of **3** with $HBF_4\cdot Et_2O$ occurs cleanly and without observable intermediates to give $H_2Ru_3(CO)_9(\mu_3\text{-}\eta^2\text{-}CHC(O)CH_3)$, which has been previously synthesized by an alternate route.[3] Similarly treatment of **3** with DCl pro-

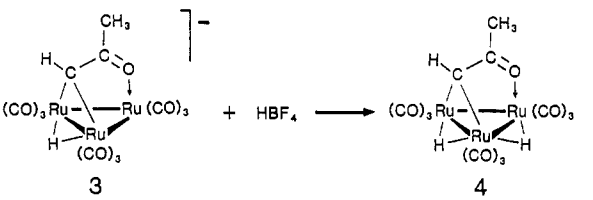

(8)

duces **4**-d_1 initially, although under these conditions the cluster rapidly eliminates acetone-d_1 (eq 9). Apparently

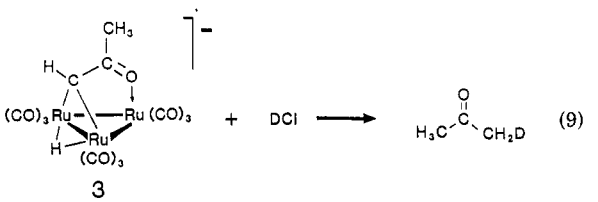

(9)

the presence of the halogen promotes the elimination reaction, as we do not observe the evolution of acetone from **4** in the absence of Cl^- or in the presence of BF_4^-. Equations 5 and 9 represent the conversion of a capping $CC(O)CH_3$ ligand into acetone. Although this process occurs

(17) (a) Azam, K. A.; Deeming, A. J.; Rothwell, I. P. *J. Chem. Soc., Dalton Trans.* **1981**, 91. (b) Azam, K. A.; Deeming, A. J.; Rothwell, I. P.; Hursthouse, M. B.; Backer-Dirks, J. D. J. *J. Chem. Soc., Dalton Trans.* **1981**, 2039. (c) Johnson, B. F. G.; Lewis, J.; Nelson, W. J. H.; Nicholls, J. N.; Vargas, M. D.; Braga, D.; Henrick, K.; McPartlin, M. *J. Chem. Soc., Dalton Trans.* **1984**, 1809. (d) Mayr, A.; Lin, Y. C.; Boag, N. M.; Kampe, C. E.; Knobler, C. B.; Kaesz, H. D. *Inorg. Chem.* **1984**, *23*, 4640. (e) Jensen, C. M.; Knobler, C. B.; Kaesz, H. D. *J. Am. Chem. Soc.* **1984**, *106*, 5926. (f) Jensen, C. M.; Chen, Y. J.; Kaesz, H. D. *J. Am. Chem. Soc.* **1984**, *106*, 4046. (g) Friedman, A. E.; Ford, P. C. *J. Am. Chem. Soc.* **1986**, *108*, 7851.

(18) Burdon, J.; Price, R. C. *J. Chem. Soc., Chem. Commun.* **1986**, 893.
(19) Seyferth, D.; Nestle, M. O. *J. Am. Chem. Soc.* **1981**, *103*, 3320.

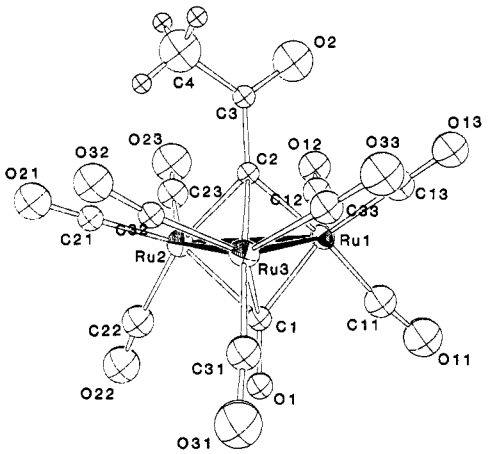

Figure 5. ORTEP drawing of the molecular structure of $[Ru_3(CO)_9(\mu_3\text{-}CO)(\mu_3\text{-}CC(O)CH_3)]^-$ (1). Isotropic (all carbon and oxygen atoms) and anisotropic (Ru1, Ru2, and Ru3) thermal ellipsoids are drawn at the 50% probability level.

via species **3** and **4** which contain O-bonded moieties, the O→Ru interaction is not strong enough to effect C–O scission in this instance.

We have also observed very slow evolution of acetone from the equilibrium mixture of **1** and **2**. Adventitious water appears to act as a proton source because addition of D_2O to the equilibrium mixture of $[Ru_3(CO)_9(\mu_3\text{-}CO)(\mu_3\text{-}CC(O)CH_3)]^-$ and $[Ru_3(CO)_7(\mu\text{-}CO)_3(\mu_2\text{-}\eta^2\text{-}CH_3C(O)CCO)]^-$ under CO leads to production of acetone-d_3. The primary cluster product is $Ru_3(CO)_{12}$, and the reaction of **1** with excess H_2O is exceedingly slow in the absence of CO. We have not investigated this reaction in detail.

Solid-State Structure of $[Ru_3(CO)_9(\mu_3\text{-}CO)(\mu_3\text{-}CC(O)CH_3)]^-$ (1). The spectroscopic characterization of **1** has been reported.[3] Except for an anomalously high-field ^{13}C NMR shift for the apical carbon of the $C\text{–}C(O)CH_3$ moiety (191.8 ppm) the spectroscopic data are consistent with the formulation of $[Ru_3(CO)_9(\mu_3\text{-}CO)(\mu_3\text{-}CC(O)CH_3)]^-$. In an attempt to better understand the reactivity of this cluster, a single-crystal X-ray structure was determined. The benzyltrimethylammonium salt of **1** is well-behaved in the solid state, with no close intermolecular contacts and no extraneous solvent molecules. The metal cluster consists of nine terminally bound carbonyl ligands and one face-capping CO. The opposite face of the metal triangle is capped by the acetylmethylidyne ligand, as shown in Figure 5. Tables I–III contain the crystallographic collection parameters, relevant bond distances and angles, and atomic coordinates for $[Ru_3(CO)_9(\mu_3\text{-}CO)(\mu_3\text{-}CC(O)CH_3)]^-$ (**4**).

The cluster molecule contains an approximate noncrystallographically imposed mirror plane containing all non-hydrogen atoms of the capping acetyl ligand and Ru1 and bisecting the Ru2–Ru3 vector. The C–C and C–O bond distances of the $\mu_3\text{-}CC(O)CH_3$ group are within error of those of acetone,[11] and the apical carbon C2 is symmetrically capping the Ru_3 triangle. The C2–C3 vector is nearly perpendicular to the plane of the metals, with a length (1.43 (3) Å) in between and within error of typical C–C single and double bond distances.[11] The Ru–Ru bond distances are typical of those found in other trinuclear ruthenium clusters with capping ligands such as $Ru_3(CO)_9(\mu_3\text{-}CO)(\mu_3\text{-}C{=}C(OCH_3)$[3] and are slightly shorter than those of $Ru_3(CO)_{12}$,[12] as would be expected from the presence of the capping groups in **1**.

Although in its reactions the ketonic oxygen atom of $[Ru_3(CO)_9(\mu_3\text{-}CO)(\mu_3\text{-}CC(O)CH_3)]^-$ shows an affinity for a metal center, the solid-state structure of the cluster gives little indication of this. The capping $\mu_3\text{-}C\text{-}C(O)CH_3$ moiety is disposed in a perpendicular bonding arrangement on **1** (Figure 5), thus although the oxygen atom of the acetyl is directly over Ru1, there is no discernible tilt of the ligand toward that metal. We have previously reported that the addition of $CH_3SO_3CF_3$ to **1** yields the vinylidene $[Ru_3(CO)_9(\mu_3\text{-}CO)(\mu_3\text{-}C{=}C(OCH_3)CH_3]$ (**6**) (Scheme I), which was crystallographically characterized.[3] The molecular structures of **1** and **6** are remarkably similar, the main difference lying in the relative dispositions of the capping vinyl and alkyl groups. The vinyl C=C moiety of **6** is tilted toward a metal vertex slightly (27° with respect to the vertical) while the C—C vector of **1** is perpendicular to the trimetallic framework. The anomalous position of the apical carbon resonance in the ^{13}C NMR spectrum of **1** (191.8 ppm) lies between the corresponding resonance of the μ_3-vinylidene **6** (168.7 ppm) and the typical range of μ_3-alkylidyne resonances (250–350 ppm).[13] Thus it may be appropriate to describe the electronic structure of $[Ru_3(CO)_9(\mu_3\text{-}CO)(\mu_3\text{-}CC(O)CH_3)]^-$ in terms of a valence isomerism (eq 10) which would impart more of a vinylic character to the $\mu_3\text{-}CC(O)CH_3$ group.

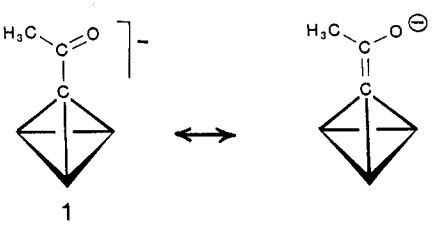

1 (10)

Table III. Positional Parameters for $[PhCH_2NMe_3][Ru_3(CO)_9(\mu_3\text{-}CO)(\mu_3\text{-}CC(O)CH_3)]$ (1)

atom	*x*	*y*	*z*
Ru1	0.3357 (2)	0.2274 (1)	0.2343 (2)
Ru2	0.2242 (2)	0.1199 (1)	0.2182 (2)
Ru3	0.2464 (2)	0.1802 (1)	0.4799 (2)
O1	0.428 (1)	0.1081 (8)	0.364 (2)
O2	0.118 (2)	0.301 (1)	0.189 (3)
O11	0.551 (2)	0.244 (1)	0.210 (3)
O12	0.297 (2)	0.251 (1)	−0.088 (3)
O13	0.322 (2)	0.364 (1)	0.337 (2)
O21	0.045 (2)	0.054 (1)	0.329 (2)
O22	0.326 (2)	−0.006 (1)	0.165 (3)
O23	0.155 (2)	0.138 (1)	−0.093 (3)
O31	0.365 (2)	0.114 (1)	0.704 (3)
O32	0.055 (2)	0.135 (1)	0.606 (2)
O33	0.242 (2)	0.308 (1)	0.623 (2)
N1	−0.409 (2)	0.063 (1)	0.047 (2)
C1	0.356 (2)	0.144 (1)	0.339 (3)
C2	0.193 (2)	0.213 (1)	0.288 (3)
C3	0.112 (2)	0.250 (1)	0.249 (3)
C4	0.011 (3)	0.232 (2)	0.296 (4)
C5	−0.428 (2)	0.006 (1)	0.131 (3)
C6	−0.496 (2)	0.088 (1)	−0.016 (4)
C7	−0.362 (2)	0.112 (1)	0.137 (3)
C8	−0.342 (2)	0.052 (1)	−0.085 (3)
C11	0.468 (2)	0.233 (2)	0.214 (4)
C12	0.312 (2)	0.241 (1)	0.029 (3)
C13	0.327 (2)	0.311 (1)	0.300 (3)
C21	0.113 (2)	0.079 (1)	0.291 (3)
C22	0.285 (2)	0.037 (1)	0.184 (3)
C23	0.183 (2)	0.128 (1)	0.027 (4)
C31	0.318 (2)	0.143 (1)	0.626 (3)
C32	0.129 (2)	0.149 (1)	0.562 (3)
C33	0.244 (2)	0.259 (1)	0.573 (3)
C41	−0.238 (2)	0.034 (1)	−0.043 (3)
C42	−0.170 (2)	0.076 (1)	−0.019 (4)
C43	−0.079 (2)	0.054 (1)	0.016 (3)
C44	−0.056 (2)	−0.011 (1)	0.034 (4)
C45	−0.127 (2)	−0.054 (1)	0.008 (3)
C46	−0.222 (2)	−0.034 (1)	−0.030 (3)

Acknowledgment. This research was supported by the

NSF synthetic inorganic organometallic chemistry program.

Registry No. [PPN]·1, 110015-18-4; [$PhCH_2NMe_3$]·1, 112042-86-1; 2, 112042-85-0; 3, 112042-87-2; 4, 110015-25-3; 5, 110015-24-2.

Supplementary Material Available: Tables of anisotropic thermal parameters and bond distances and angles for [$Ru_3(CO)_9(\mu_3\text{-}CO)(\mu_3\text{-}CC(O)CH_3)]^-$ (1) and the mass spectral data for the acetone-d_1 produced from 4-d_1 (7 pages); a listing of F_o and F_c (9 pages). Ordering information is given on any current masthead page.

Weak Carbon–Carbon Bonds. Synthesis, Structure, and Reactions of 7-Methyl-1,3,5-triphenyl-2,4,9-trithia-1,3,5-tristannaadamantane

Michel Gallant,[1] Michio Kobayashi, Stéphan Latour, and James D. Wuest*

Département de Chimie, Université de Montréal, Montréal, Québec, H3C 3J7 Canada

Received August 17, 1987

7-Methyl-1,3,5-triphenyl-2,4,9-trithia-1,3,5-tristannaadamantane (1-CH_3) was synthesized to test the possibility that a carbon–methyl bond activated by three antiperiplanar carbon–tin bonds might be a reactive donor of methyl. MNDO calculations suggest that the strength of the carbon–methyl bond in compound 1-CH_3 should be about 40 kcal/mol. Nevertheless, the reactivity of this bond is not conspicuously high. This is presumably because the methyl group is neopentylic and sterically hindered and because other weak bonds in compound 1-CH_3 are even more reactive and obscure the intrinsic activation of the carbon–methyl bond by making reactions occur elsewhere.

Carbon–hydrogen bonds adjacent to properly oriented lone pairs or carbon–metal bonds are unusually weak and reactive, and compounds containing these activated carbon–hydrogen bonds are effective donors of hydrogen in redox reactions.[2-4] For example, stannaadamantane 1-H

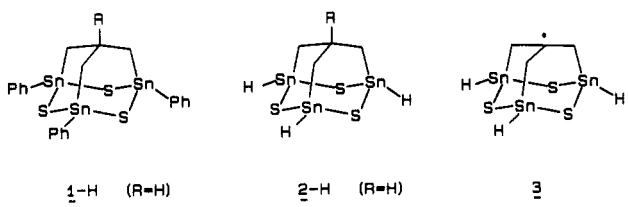

1-H (R=H) 2-H (R=H) 3

1-CH_3 (R=CH_3) 2-CH_3 (R=CH_3)

incorporates a carbon–hydrogen bond activated by three antiperiplanar carbon–tin bonds.[3] Its strength, calculated to be 61 kcal/mol,[5a] is much lower than that of the methine carbon–hydrogen bonds in isobutane (95 kcal/mol)[6] or adamantane (99 kcal/mol)[6] and appears to be even lower than that of a typical tin–hydrogen bond (72 kcal/mol in trimethylstannane).[7] As a result, abstraction of hydrogen from stannaadamantane 1-H by alkyl radicals is generally quite exothermic, allowing compound 1-H to act like a tin hydride and reduce activated halides to the corresponding hydrocarbons.[3a]

Table I. Average Bond Lengths (Å) and Bond Angles (deg) Observed for Stannaadamantane 1-H[3c] and Calculated for Stannaadamantanes 2-H and 2-CH_3 Using MNDO[5c]

parameter	1-H	2-H	2-CH_3
Sn–S	2.408	2.279	2.277
Sn–C	2.153	2.096	2.099
CH_2–C	1.529	1.546	1.558
CH_3–C			1.570
S–Sn–S	108.7	109.1	109.2
S–Sn–C	108.8	108.2	108.7
Sn–CH_2–C	119.3	118.2	120.4
CH_2–C–CH_2	114.1	113.9	111.7
Sn–S–Sn	94.3	98.1	97.2

The use of properly oriented lone pairs or carbon–metal bonds to produce highly reactive carbon–hydrogen bonds is a general strategy that can be exploited to create other weak bonds as well. To test the possibility that a carbon–methyl bond activated by three antiperiplanar carbon–metal bonds might be a reactive donor of methyl, we decided to prepare methylstannaadamantane 1-CH_3 and study its structure and reactions.[8]

To help accommodate the characteristically long tin–sulfur bonds, the bridgehead carbon of stannaadamantane

(1) Fellow of the Natural Sciences and Engineering Research Council of Canada.

(2) Bachand, B.; Ramos, S. M.; Wuest, J. D. *J. Org. Chem.* **1987**, *52*, 5443–5446. Ramos, S. M.; Tarazi, M.; Wuest, J. D. *Ibid.* **1987**, *52*, 5437–5442.

(3) (a) Ducharme, Y.; Latour, S.; Wuest, J. D. *J. Am. Chem. Soc.* **1984**, *106*, 1499–1500. (b) Ducharme, Y.; Latour, S.; Wuest, J. D. *Organometallics* **1984**, *3*, 208–211. (c) Beauchamp, A. L.; Latour, S.; Olivier, M. J.; Wuest, J. D. *J. Am. Chem. Soc.* **1983**, *105*, 7778–7780.

(4) Erhardt, J. M.; Grover, E. R.; Wuest, J. D. *J. Am. Chem. Soc.* **1980**, *102*, 6365–6369. Erhardt, J. M.; Wuest, J. D. *Ibid.* **1980**, *102*, 6363–6364.

(5) (a) Dewar, M. J. S.; Grady, G. L. *Organometallics* **1985**, *4*, 1327–1329. (b) Dewar, M. J. S.; Grady, G. L.; Kuhn, D. R.; Merz, K. M., Jr. *J. Am. Chem. Soc.* **1984**, *106*, 6773–6777. Dewar, M. J. S.; Grady, G. L.; Stewart, J. J. P. *Ibid.* **1984**, *106*, 6771–6773. (c) Dewar, M. J. S.; Thiel, W. *Ibid.* **1977**, *99*, 4907–4917. Dewar, M. J. S.; Thiel, W. *Ibid.* **1977**, *99*, 4899–4907.

(6) Kruppa, G. H.; Beauchamp, J. L. *J. Am. Chem. Soc.* **1986**, *108*, 2162–2169.

(7) Smith, G. P.; Patrick, R. *Int. J. Chem. Kinet.* **1983**, *15*, 167–185. Jackson, R. A. *J. Organomet. Chem.* **1979**, *166*, 17–19.

(8) For other recent studies of organometallic derivatives of adamantane, see: Haas, A.; Kutsch, H.-J.; Krüger, C. *Chem. Ber.* **1987**, *120*, 1045–1048. Ellermann, J.; Veit, A. *Z. Naturforsch., B: Anorg. Chem., Org. Chem.* **1985**, *40B*, 948–953. Boudjouk, P.; Kapfer, C. A.; Cunico, R. F. *Organometallics* **1983**, *2*, 336–343. Fritz, G.; Gompper, K. *Z. Anorg. Allg. Chem.* **1981**, *478*, 94–96. Mironov, V. F.; Gar, T. K.; Fedotov, N. S.; Evert, G. E. *Usp. Khim.* **1981**, *50*, 485–521.

0276-7333/88/2307-0736$01.50/0 © 1988 American Chemical Society